Original papers

Rice blast recognition based on principal component analysis and neural network

Maohua Xiao[a,b], You Ma[a], Zhixiang Feng[a], Ziang Deng[a], Shishuang Hou[a], Lei Shu[a,c], ZhiXiong Lu[a,*]

[a] College of Engineering, Nanjing Agricultural University, Nanjing 210031, China
[b] Faculty of Engineering and the Environment, University of Southampton, SO17 1BJ, UK
[c] School of Engineering, University of Lincoln, Lincoln, UK

ABSTRACT

Based on principal component analysis and back propagation neural network (PCA-BP), a rice blast recognition method was proposed to solve the problems of low accuracy, inefficiency and subjectivity of artificial recognition of rice blast. First, image of harvested lesion was processed, with 6 color features, 10 morphological features, and 5 texture features of each lesion were extracted. Secondly, stepwise regression analysis was used to analyze the correlation between the characteristic parameters. The results showed a linear correlation. Then, the principal component analysis (PCA) method was used to reduce the dimension linearly, to map 21 features into 6 comprehensive features as input parameters. Finally a 6-11-4, 3-layer back propagation (BP) neural network identification model was constructed for the classification and recognition of the lesion. The experimental results show that the average recognition rate of rice blast based on principal component analysis and BP neural network is 95.83%, which is 7.5% higher than the average recognition rate using BP neural network and 2.5% higher than the existing SVM method with high accuracy in identifying rice blast. It can identify rice blast quickly and effectively.

1. Introduction

Rice blast is one of the most destructive rice diseases that are caused by the Ascomycetes Manaporthe grisea (Hebert Barr) and occur extensively around the world (Kumar et al., 2016). It not only leads to loss of rice yield, but also seriously reduces the quality of rice (Joshi and Jadhav, 2016; Huang et al., 2015). Fig. 1 shows four different types of rice blast lesion. Thus, preventing and treating rice blast has become a global issue of wide concern and research. At present, the chemical control is the most effective measure for prevention and treatment of rice blast, including using chemicals to sterilize the seeds before sowing, and spraying pesticides at the various growth stages that easy to contract rice blast or according to the disease degree of rice blast (Sha et al., 2016). However, one drawback with chemical control is that the overuse of pesticides would have an adverse effect on the environment (air, water and soil) and human health. To address the problem above, we must obtain the crops growth information quickly and accurately, timely diagnose the etiology and degree of injured crops, and then use the appropriate pesticides and dosage according to indications. All of these are relied on the effective recognition and

diagnosis method of rice blast. To the best of our knowledge, the rice blast is usually identified by observing the shape and color of the lesion, and then determined the type of disease according to the disease book. Obvious, this traditional method is subjective and requires high professional knowledge and rich experience. Moreover, its identification accuracy and efficiency is also relatively low. Therefore, a simple and fast identification method with high accuracy for rice blast is urgently needed.

With the development of science and technology, computer technology has been increasingly used in the field of agricultural engineering, thereby forming a number of effective plant disease recognition methods (Abdullakasim et al., 2015; Hu et al., 2016; Baldi et al., 2017; Chaki et al., 2015). Among these methods, the image recognition of plant diseases has attracted much attention. Generally, this approach is firstly to extract the characteristic feature information from the diseased regions in the obtained images by using image processing techniques, and then to achieve disease recognition by using pattern recognition methods (e.g. discriminant analysis, neural networks and support vector machine) (Shi et al., 2017; Wang et al., 2012; Bakhshipour and Jafari, 2018), which could get a large amount of

---

(a) Acute type lesions　　(b) White spots type lesions　　(c) Chronic type lesions　　(d) Brown spots type lesions.
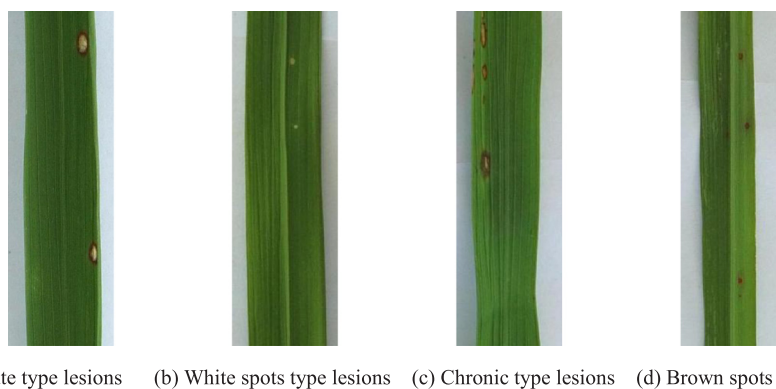
Fig. 1. Rice blast disease graph. (a) Acute type lesions (b) White spots type lesions (c) Chronic type lesions (d) Brown spots type lesions.

information quickly, and accurately distinguish the nuances to avoid the errors caused by human factors. It has been demonstrated that a lot of plant diseases have been successfully identified via using the image processing techniques and neural network methods, such as the apple disease (Boniecki et al., 2015), cucumber lesion (Jia and Ji, 2013); maize diseasep (Cao et al., 2012), and other plant leaf diseases (Chouhan et al., 2018). Although the identification of rice blast using image processing techniques and multi-layer perceived neural network have been also reported (Liu and Zhou, 2009); the research on the identification of different types of lesions of rice blast is still not enough. In the meantime, most of the studies above directly input the obtained eigenvalues into the neural network classifier for feature training and classification. If there is some correlation between certain features or the contribution of features to the recognition rate is not large, the recognition time and accuracy will be affected. Selecting features with large contribution rate and small correlation between features can reduce the redundant data and shorten the time of data processing and recognition. Due to the large number of features and the insignificant correlation between features, direct manual selection may not be good. Existing feature extraction and dimensionality reduction techniques include linear methods (Zabalza et al., 2014; Zabalza et al., 2014) (such as principal component analysis, etc.) and nonlinear methods (such as local linear embedding Huang et al., 2012, etc.). Perform correlation analysis on the extracted feature data and find that the data are linearly related, therefore the principal component analysis method was chosen to reduce the dimension of the data in this research.

In view of the above problems, this paper presents a method combining image processing technology, principal component analysis and BP neural network (PCA-BP) to identify four different types of rice blast lesions. Firstly, the lesion image was obtained by camera and the lesion image was preprocessed. Then the lesion morphology, color and texture features were extracted. After that, the PCA was used to reduce the dimension of the feature vector. Finally, the dimensionality-reduced feature vectors were input to the neural network for lesion classification. The experimental results show that the average accuracy of PCA-BP method is 95.83%, which is higher than that of direct recognition by BP neural network (88.33%), and 2.5% higher than the existing SVM method with high accuracy in identifying rice blast (Zhao et al., 2013). In addition, the recognition speed is about 9 times faster than the image recognition without PCA at a relatively high recognition rate. Our findings provide a new method for the rapid and efficient identification of rice blast.

2. Lesions classification and data collection

2.1. Lesions classification

In this paper, four different types of rice blast lesions were studied. Four different types of rice blast lesion characteristics are shown in

Table 1
Four different types of rice blast lesion characteristics.

Disease name	Shape characteristics	Color and texture features
Chronic type lesions	Fusiform	Center: gray; Edge: brown; Peripheral: yellow halo
Acute type lesions	Nearly round or oval	Dark green; gray moldy layer
Brown spots type lesions	Dots	Brown
White spots type lesions	Dots	White

Table 1.

2.2. Lesion image acquisition

In this paper, all the rice disease image samples were collected under the natural environment in August 2017 in Jiangpu Experimental Base of Nanjing Agricultural University. In order to reduce the error caused by light, the image sampling was operated in 7:00 am to 10:00 pm and 4:00 pm to 6:00 pm, the image was taken using a Zen Z3 camera (resolution 4000×3000) in single focal length mode to shoot the rice leaves. The camera is about 0.2 m above the sample. To get a clearer leaf image of the disease, an A4 paper was placed under the leaves to eliminate other complex background, the experiment collected a total of 387 different lesion samples including 374 valid samples. The pixel size of the image processed in the experiment was 700×200, and the image processing algorithm was implemented in Matlab 2014b. The basis for the selection of the time period for image acquisition is based on experiments conducted at 8:00 am, 10 am, 12 pm, and 2 pm, 4 pm, and 6 pm. The effect is shown in Fig. 2 after observing the effect of shooting time on the RGB channel of the same sample.

It can be seen from Fig. 2 that under different light intensities at different times, appropriate sunshading measures are taken under bright light at noon, and the RGB three-channel histograms of the same sample are different. Under the condition of avoiding strong light, the difference in histogram waveforms is not significant, and the difference in images is not significant.

3. Lesion feature extraction and correlation analysis

The color, shape, and texture of an image can be described by the relationship between the structure of the image and the color distribution, often used as feature vectors for image recognition. There are some differences in the color, morphology, and texture between the four kinds of lesions of rice blast, so the lesion color, morphological, and texture features can be extracted as the eigenvectors for the identification of the four kinds of lesions.
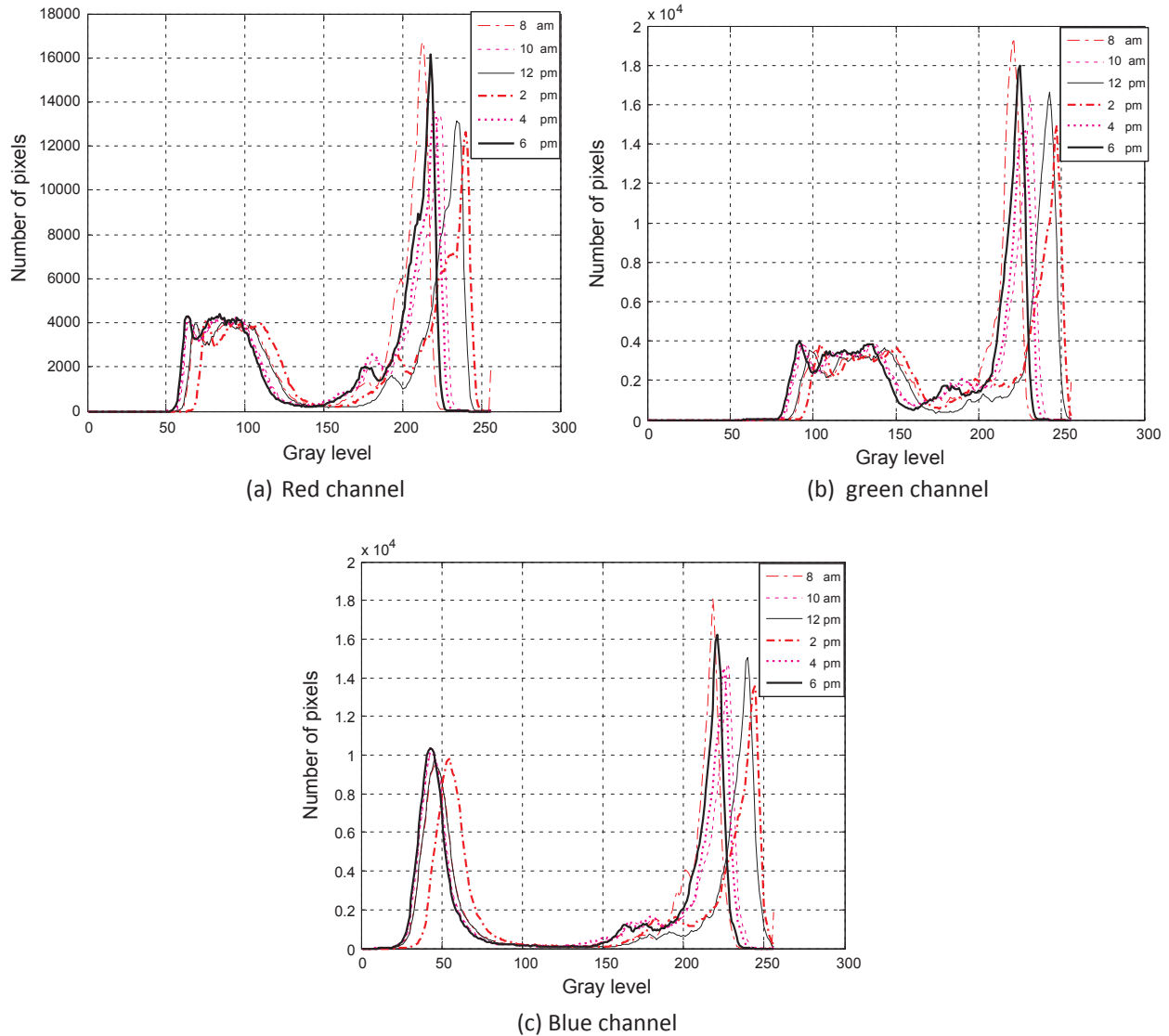
(a) Red channel

(b) green channel

(c) Blue channel

Fig. 2. R, G, B three-channel gray level distribution images.

3.1. Color feature extraction

In digital image processing, the most fundamental sampling color coordinate system is RGB, but R, G, B three components are greatly affected by the lighting (Liu and Zhou, 2009). As the samples were collected under natural light, and greatly affected by the light, R, G, B components were not chosen as color characteristics. RGB color space was converted to HSI and YCbCr color space with independent color and brightness information through color space conversion, which can effectively restrain noise and reduce the influence of uneven illumination (Qi et al., 2006). In this study, H, S, I, Y, Cb, and Cr were selected as the color eigenvalues for identification. Due to space limitations, only HIS and YcbCr spatial map and their components of the acute type lesion were given, as shown in Figs. 3 and 4.

3.2. Morphological feature extraction

After analyzing the histograms of the color components R, G, and B in the experiment, the G-B, R-G, and 2G-R-B color component combinations were selected for image processing. First, each color component combination was median filtered, then the image was segmented using the maximum interclass variance method (OSTU) (Sha et al., 2016) to get the binary image. As shown in Fig. 5. It was found that only the

lesion area was found after R-G segmentation, which was convenient for morphological feature extraction and segmentation. Finally, the R-G component combination was chosen for analysis.

The binarized image obtained by image segmentation was subjected to morphological processing. Morphological processing can eliminate some isolated dots, fill holes, smooth the edges, and reduce the interference of small dots on the analysis results. Morphologically treated lesion images were regionally marked. Area labeling refers to attaching the same label to the connected pixels and attaching different labels to different connected components (Zhao et al., 2008). Regional features and boundary features can be extracted separately by region markers to calculate morphological parameters of each lesion.

In this paper, 10 morphological features including area (the number of pixels in lesion area), perimeter (the number of contour pixels in lesion area), eccentricity, minimum circumscribed rectangle area (in the pixel sense), ovality, rectangularity, the long axis, short axis, and the ratio of long axis to short axis of the equivalent ellipse, and complexity were extracted. Among them, the ovality, the rectangularity, and the complexity were calculated by (1)–(3).

Ovality: $E = \dfrac{a-b}{a}$ (1)
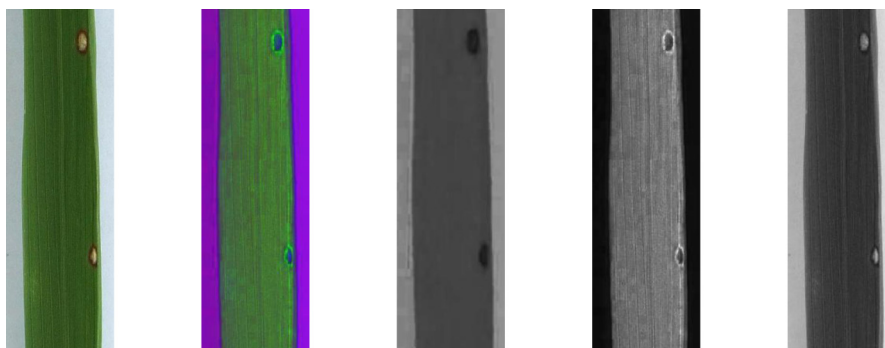
(a) Original graph (b) HSI space graph (c) H component graph (d) S component graph (e) I component graph

Fig. 3. HSI and H, S, I component graphs of acute lesions original graph. (a) Original graph (b) HSI space graph (c) H component graph (d) S component graph (e) I component graph.

Rectangularity: $R_{sq} = \dfrac{A}{SMER}$ (2)

Complexity: $C = \dfrac{P^2}{A}$ (3)

In (1)–(3), a and b respectively are the major and minor axis lengths of the ellipse equivalent to the lesion area in the pixel sense, A is the lesion area, P is the circumference, and SMER is the smallest circumscribed rectangle area.

3.3. Texture feature extraction

Rice lesion texture is an important index to distinguish the type of rice lesion, while the gray level co-occurrence matrix can reflect the main texture features of the image. Set to $f(x, y)$ as a two-dimensional digital image, image size $M \times N$, gray level L. Assuming that (x_1, y_1) and (x_2, y_2) are two pixels in $f(x, y)$, the distance is d and the angle between the two and the ordinate is θ, then a gray level co-occurrence matrix $P(i, j|d, \theta)$ is obtained (Tang et al., 2008):

$$P(i, j|d, \theta) = \#\{(x_1, y_1), (x_2, y_2) \in M \times N|d, \theta, f(x_1, y_1) = i, f(x_2, y_2) = j\}$$
(4)

where # {x} represents the number of cells in the curly brackets, θ is the span value, the interval is generally limited to 45°.

In this paper, five parameters including entropy (ENT), angular second moment (ASM), contrast (CON), correlation (COR), and inverse difference moment (IDM) were selected as the texture features for lesion recognition. Eqs. (5)–(9) are formulas for calculating the five parameters:

Entropy: $ENT = -\sum\limits_{i=1}^{L}\sum\limits_{j=1}^{L} P(i, j)\log P(i, j)$ (5)

Angular second moment: $ASM = \sum\limits_{i=1}^{L}\sum\limits_{j=1}^{L} (P(i, j))^2$ (6)

Contrast: $CON = \sum\limits_{i=1}^{L}\sum\limits_{j=1}^{L} (i-j)^2 P(i, j)$ (7)

Correlation: $COR = \dfrac{\sum\limits_{i=1}^{L}\sum\limits_{j=1}^{L} i \times j \times P(i, j) - \mu_x\mu_y}{\sigma_x\sigma_y}$ (8)

Inversedifference moment: $IDM = \sum\limits_{i=1}^{L}\sum\limits_{j=1}^{L} \dfrac{p(i, j)}{[1 + (i-j)^2]}$ (9)

where μ_x, μ_y, σ_x, and σ_y are the sum of expected and variance values for the row and column matrix elements, respectively.

Table 2 shows the total characteristic values shown above.

3.4. Correlation analysis

In this study, stepwise regression analysis method (Li, 2004) was used to perform correlation analysis on feature data. Each feature value was set as the dependent variable, and the remaining feature values were set as independent variables, then the correlation between the feature values was analyzed. The analysis results are shown in Fig. 6.

As can be seen from Fig. 6, except for the correlation of Rectangularity and Contrast being less than 70%, the correlations of other features are all above 80%, indicating that there is a strong correlation between features. Therefore PCA can be used to perform linear
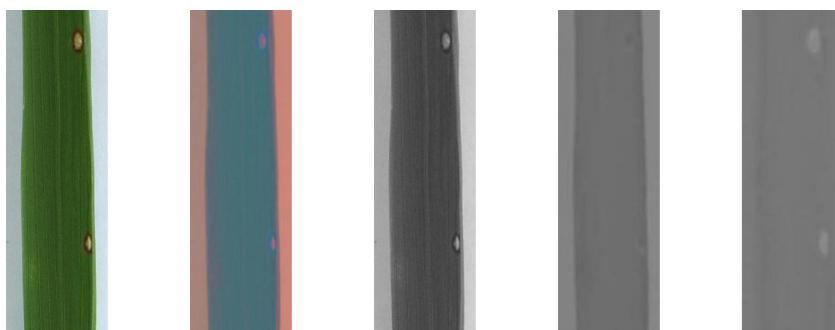
(a) Original graph (b) YCbCr space graph (c) Y component graph (d) Cb component graph(e) Cr component graph

Fig. 4. YCbCr and Y, Cb, Cr component graphs of acute lesions. (a) Original graph (b) YCbCr space graph (c) Y component graph (d) Cb component graph (e) Cr component graph.
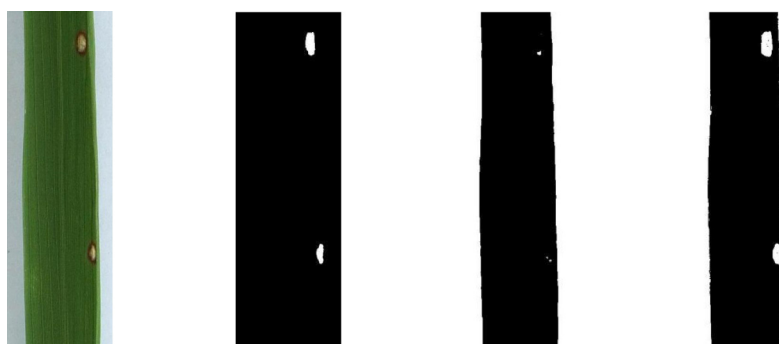
(a) Original graph   (b) R-G segmentation graph   (c) G-B segmentation graph (d) 2G-R-B segmentation graph

Fig. 5. Acute type lesion combination of color components segmentation renderings. (a) Original graph (b) R-G segmentation graph (c) G-B segmentation graph (d) 2G-R-B segmentation graph.

dimensionality reduction.

4. Rice blast lesion recognition

4.1. Principal component analysis

In this study, a total of 21 color, morphological, and texture features were extracted from rice blast. Some of these features have obvious differences among the four kinds of lesions, some of the eigenvalues do not change obviously, and some of the features are related to each other. Selecting features that have a large contribution to recognition and small correlations helps to reduce redundant data and reduce algorithm processing time. Due to the relatively large number of features, the direct artificial selection effect is not ideal and subjective strong.

The Principal component analysis (PCA) is an important method of multivariate statistical analysis (Zhao et al., 2014). By studying the internal structure of the index system and mapping the multiple features into a few comprehensive features according to the principle of maximum variance, dimensionality reduction can be realized, transforming strongly correlated variables into variables that are independent or irrelevant to each other. If the number of principal components is too small, the feature information will be lost and the recognition rate will be reduced. However, if the factor is too much, redundant data will be introduced to cause supersaturation, which will affect the accuracy of recognition. Therefore, a reasonable number of principal component factors should be selected. In practice, it is common to take the principal components that contribute a large amount of the first few deviations, which can not only reduce the information loss but also reduce the variables and reduce the correlation between the variables. Generally recommended cumulative contribution rate of 80% or more is appropriate (Liu, 2014).

In this study, MATLAB 2014b software was used to carry out principal component analysis. Table 3 shows the eigenvalues and their respective contribution rates of the first six principal components. The cumulative contribution rates of the principal components and the contribution rates of each principal components are shown in Fig. 7.

As shown in Table 3 and Fig. 7, the contribution rate of the first principal component is 38.79%, the cumulative contribution rate of the first two principal components is 61.48%, the cumulative contribution rate of the first three principal component is 74.26%, the cumulative contribution rate of the first four principal component is 83.95%, the cumulative contribution rate of the first five principal components is 89.84%, and the cumulative contribution rate of the first six principal components is 94.52%. The number of principal components in the selection is determined by the cumulative contribution of principal components, recognition accuracy, and recognition time.

4.2. Blast disease identification based on BP neural network

BP neural network is a multi-layer feedforward neural network with three or more layers, which consists of input layer, hidden layer, and output layer. In a given input mode and expected response, according to the principle of reducing the error between output and the actual, reverse spread to amend the weight of each connection. The constant adjustment of the weights makes the correct rate of the network esponse to the input mode (Si and Sun, 2015).

In this study, BP neural network used a single implicit structure with one middle layer. The transfer function of the hidden and output layer both is the sigmoid transfer function logsig. The number of neurons in hidden layer based on empirical formula $\sqrt{(m+n)}+a$ (m is the number of input neurons, n is the number of output neurons, a is a constant of 1–10) and multiple experiments. Due to the need to identify four different types of rice blast lesions in this study, the number of neurons in the output layer is 4, the results of the output including 1000, 0100, 0010, and 0001, which respectively represent the acute type lesions, chronic type lesions, brown-point lesions, and white-point lesions. The lesion identification flowchart is shown in Fig. 8.

A total of 240 lesions of each 60 were selected as a training sample, and then 30 of each lesion were selected as a test sample for network testing. Taking the principal components with different number as the input of BP neural network, the accuracy of recognition and recognition time under different number of principal components were obtained (as
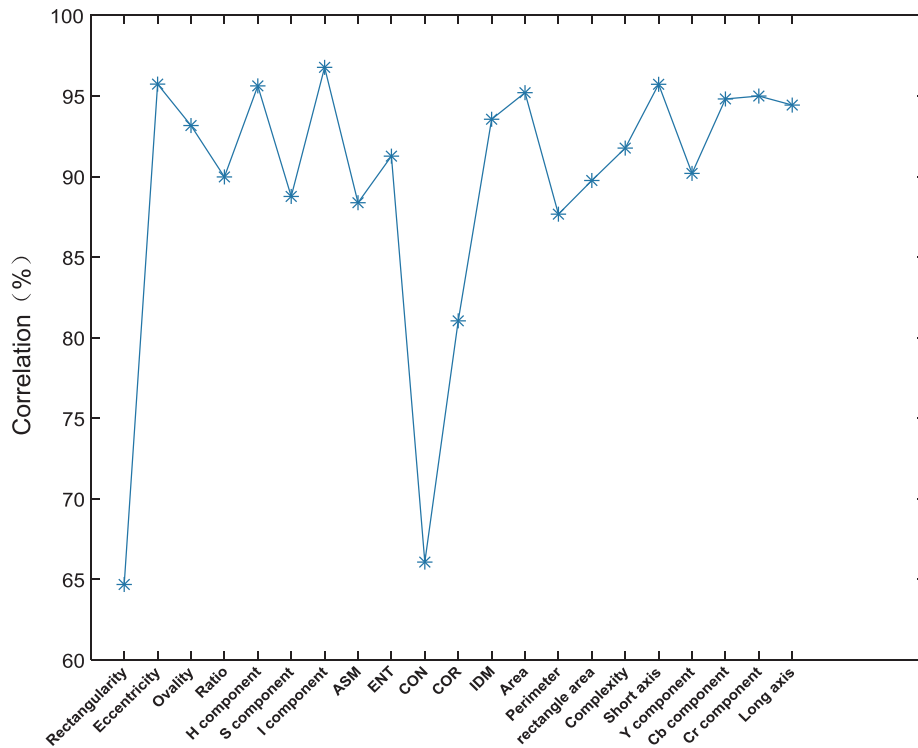
Table 2
Eigenvalue table.

Eigenvalue				
Color features		Morphological features		Texture features
H component	Y component	Long axis	Eccentricity	Entropy
S component	Cb component	Short axis	Minimum circumscribed rectangle area	Angular second moment
I component	Cr component	Ratio of long axis to short axis	Ovality,	Contrast
		Area	Rectangularity	Correlation
		Perimeter	Complexity	Inverse difference moment

Fig. 6. Analysis chart of correlation between features. Note: Ratio is "Ratio of long axis to short axis", rectangle area is "Minimum circumscribed rectangle area".

Table 3
Eigenvalues and contributions.

Principal components	Eigenvalues	Contributions
1	8.14659	38.793%
2	4.76508	22.691%
3	2.68311	12.777%
4	2.03435	9.687%
5	1.23614	5.886%
6	0.98301	4.681%
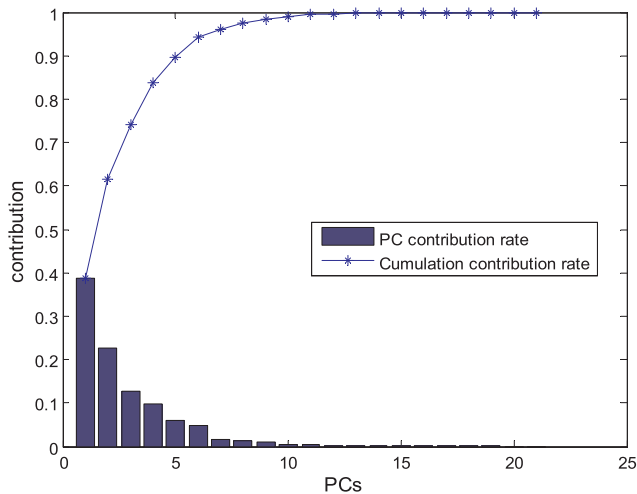
Fig. 7. Principal component analysis chart.

Fig. 8. Lesion identification flowchart.

rate. Moreover, the cumulative contribution rate of the first 6 principal components is 94.52%, which can better maintain the original characteristics. Considering the factors above comprehensively, the 6 principal components were selected to recognize. Therefore the number of neurons in the input layer is 6. Finally, this study confirmed the BP neural network structure as 6−11−4. The optimal structure of BP neural network was based on the empirical formula. By comparing the average accurate recognition results of 4 kinds of lesions of different hidden layers, the recognition result is shown in Fig. 10.

It can be seen from the figure that when the number of hidden layers is 11, only the number of accurate identification of acute lesions is one

shown in Fig. 9).

From the figure, it can be seen that the recognition accuracy reached 95.83% when selecting the first six principal components, only 0.84% lower than the best recognition 96.67%, but the recognition speed is at least two times faster than the speed at the best recognition
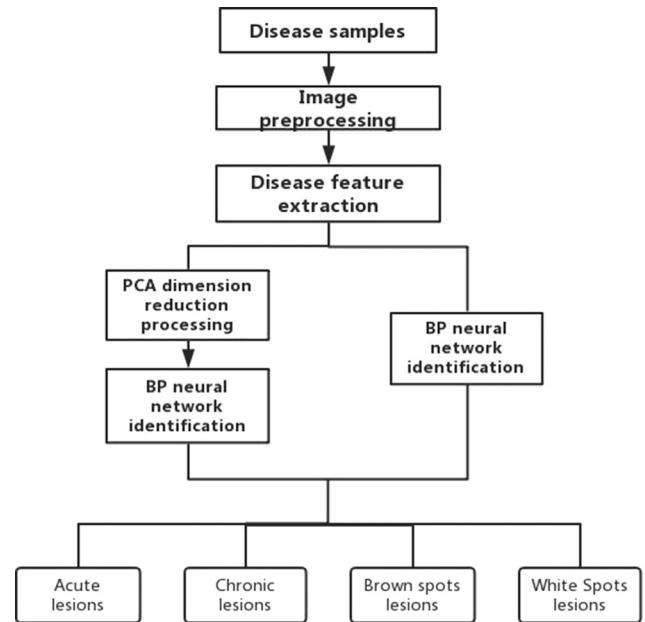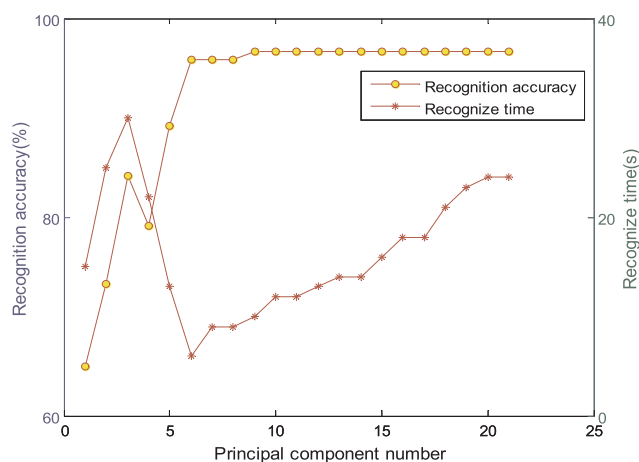
Fig. 9. The recognition effect graph of different number of principal components.
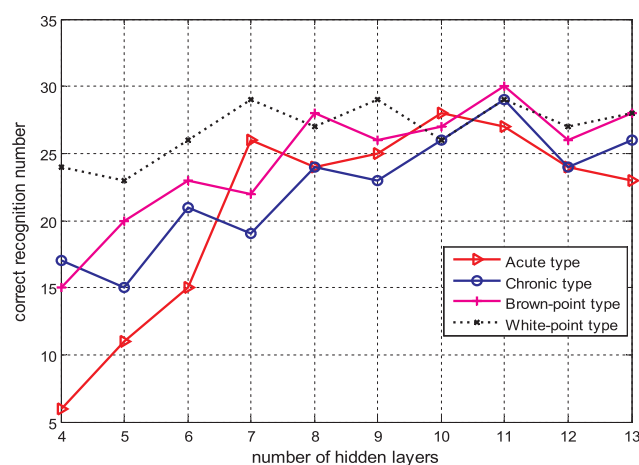

Fig. 10. Recognition renderings of different hidden layers.

less than when the hidden layer is 10, the other three kinds of lesion identification numbers are the most. The average recognition accuracy of the four kinds of lesions is the highest, reaching 95.83%.

The 6 principal components after dimensionality reduction and the 21 features without dimensionality reduction were tested respectively as input of BP neural network. The results showed that when input 6 principal components, after 84 iterations the mean square error reached the required goal error 0.001, which used time of 6 s, and the average recognition rate reached 95.83%. However BP neural network test required 437 iterations to hit the target error requirement, with a time of 55 s, and the average recognition rate reached 88.33%, the structure of BP network without dimensionality reduction is 21−14−4.Two methods were used to test the correctness of 120 lesions, the results of which are shown in Tables 4 and 5.

As can be seen from Tables 4 and 5, the average recognition rates of blast lesion using PCA-BP neural network and BP neural network are

95.83% and 88.33% respectively, the accuracy of using PCA-BP compared with using BP network increased by 7.5%. Comparison of the results of the two tables shows that the two both are easy to identify as chronic type of lesion when recognizing the acute type of lesion. After observing the wrong type of acute lesions identified, it was found that the misrecognized acute lesions and chronic lesions were very close in shape and color, since the acute type is gradually similar in morphology and color to the chronic type. BP neural network test identified two false positives whereas PCA-BP misidentified only one when identifying chronic lesions. Three errors were observed in the BP neural network when identifying the brown-point type, whereas PCA-BP identified with no error. It is because after dimensionality analysis, the correlation between the components is small, making PCA-BP better in recognition, but the two methods are both easy to identify white-point type lesion as acute type lesion. Lesions under certain environmental conditions can be transformed into acute type lesions. The two lesions in morphology and color characteristics are similar, resulting in classification misjudgment. From the overall recognition effect, the PCA-BP method can optimize the data to a certain extent and improve the recognition accuracy and efficiency.

In this study, PCA-SVM and segmented-PCA-BP neural networks were also compared. The PCA-SVM recognition results were shown in Table 6. In the segmented-PCA(Ren et al., 2014) study, 21 features were divided into three segments, each segment has 7 parameters. The three segment parameters were processed for data optimization. Four diseases were identified under the different number of principal components. The average disease recognition rate was obtained. The identification results are shown in Fig. 11.

It can be seen from the figure that the seven factors in the first stage have the greatest contribution to the recognition effect. When the six principal components are selected, the average recognition effect is the best. The recognition rate is 92.5%, but it is 3.33% lower than that of PCA-BP. The average recognition rate of PCA-SVM is 93.33%, which is 2.5% lower than PCA-BP. Therefore, PCA-BP was used for disease identification in this study.

5. Conclusion

Four rice blast diseases were treated by image processing technology to obtain the color, morphological, and texture features of lesion. Combining with principal component analysis and BP neural network, four identification models of rice blast lesion were established to rapidly identify the lesion. Firstly, 6 color features, 10 morphological features and 5 texture features of each lesion were extracted, and then principal component analysis method was used to reduce the dimension to get 6 principal component factors which were input in BP neural network. Finally 6−11−4 3-layer neural network structure constructed classified and identified the rice blast lesion. The average recognition rate reached 95.83%, increased by 7.5% compared with using BP neural network recognition method.

In summary, the PCA-BP method proposed in this paper can optimize the characteristic parameters to facilitate the rapid and efficient identification of rice blast disease, but there are still some shortcomings in the identification of lesions with similar morphology and color. Overall, the research method proposed in this paper provides a new

Table 4
The recognition results of 4 kinds of blast using PCA-BP.

Lesions category	Sample	Recognition results of test set				Recognition rate	Average recognition rate
		Acute type	Chronic type	Brown-point type	White-point type		
Acute type	30	27	3	0	0	90.00%	95.83%
Chronic type	30	1	29	0	0	96.67%	
Brown-point type	30	0	0	30	0	100%	
White-point type	30	1	0	0	29	96.67%	

Table 5
The recognition results of 4 kinds of blast using BP neural network.

Lesions category	sample	Recognition results of test set				Recognition rate	Average recognition rate
		Acute type	Chronic type	Brown-point type	White-point type		
Acute type	30	25	4	0	1	83.33%	88.33%
Chronic type	30	2	28	0	0	93.33%	
Brown-point type	30	1	2	27	0	90.00%	
White-point type	30	4	0	0	26	86.67%	

Table 6
The recognition results of 4 kinds of blast using PCA-SVM.

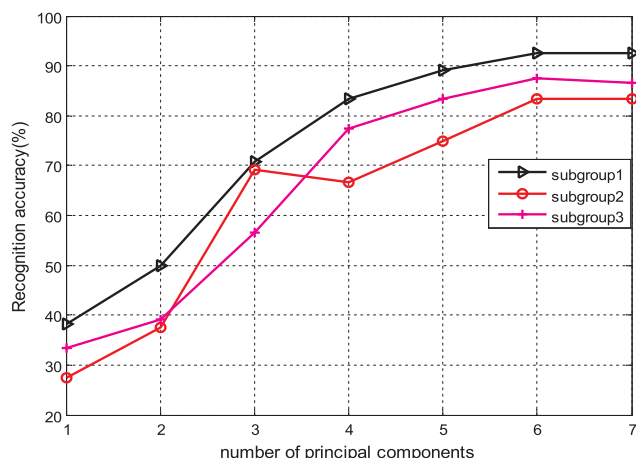| Lesions category	sample	Recognition results of test set				Recognition rate	Average recognition rate
		Acute type	Chronic type	Brown-point type	White-point type		
Acute type	30	27	3	0	0	27	90.00%
Chronic type	30	2	28	0	0	28	93.33%
Brown-point type	30	1	0	29	0	29	96.66%
White-point type	30	0	2	0	28	28	93.33%

Fig. 11. Recognition renderings of different principal component Numbers.

idea for real-time rapid identification of rice blast.

Competing interests

The authors declare that there are no competing interests regarding the publication of this paper.

Funding

Appendix A. Supplementary material

Supplementary data associated with this article can be found, in the online version, at https://doi.org/10.1016/j.compag.2018.08.028.

References

Kumar, A., Mishra, A.K., Jain, A.K., 2016. In-silico identification of inhibitors for controlling rice blast. In: 2016 International Conference on Computing for Sustainable Global Development (INDIACom), pp. 1888–1892.

Joshi AA, Jadhav BD, 2016. Monitoring and controlling rice diseases using Image processing techniques. In: 2016 International Conference on Computing, Analytics and Security Trends (CAST), pp. 471–476.

Huang, S.P., Qi, L., Ma, X., Xue, K.N., Wang, W.J., Zhu, X.Y., 2015. Hyperspectral image analysis based on BoSW model for rice panicle blast grading. Comput. Electron. Agric. 118, 167–178.

Sha, Y.X., Wang, Q., Li, Y., 2016. Screening and prevention of bacillus biocontrol against rice blast. Chinese J. Biol. Control. 32 (4), 474–484.

Abdullakasim, W., Powbunthorn, K., Unartngam, J., 2015. Detection of chlorotic cassava leaves using image processing and discriminant analysis. Thai Soc. Agric. Eng. J. 21 (2), 50–59.

Hu, Y.H., Ping, X.W., Xu, M.Z., Dan, W.X., He, Y., 2016. Detection of late blight disease on potato leaves using hyperspectral imaging technique. Spectrosc. Spect. Anal. 36 (2), 515–519.

Baldi, A., Pandolfi, C., Anna Lenzi, S.M., 2017. A leaf-based back propagation neural network for oleander (Nerium oleander L.) cultivar identification. Comput. Electron. Agric. 142, 515–520.

Chaki, J., Parekh, R., Bhattacharya, S., 2015. Plant leaf recognition using texture and shape features with neural classifiers. Pattern Recogn. Lett. 58, 61–68.

Shi, Y., Huang, W.J., Luo, J.H., Huang, L.S., Zhou, X.F., 2017. Detection and discrimination of pests and diseases in winter wheat based on spectral indices and kernel discriminant analysis. Comput. Electron. Agric. 141, 171–180.

Wang, H.G., Li, G.L., Ma, Z.H., Li, X.L., 2012. Application of neural networks to image recognition of plant diseases. Syst. Informat. (ICSAI).

Bakhshipour, A., Jafari, A., 2018. Evaluation of support vector machine and artificial neural networks in weed detection using shape features. Comput. Electron. Agric. 145, 153–160.

Boniecki, P., Koszela, K., Piekarska-Boniecka, H., Weres, J., Zaborowicz, M., Kujawa, S., Majewski, A., Raba, B., 2015. Neural identification of selected apple pests. Comput. Electron. Agric. 110, 9–16.

Jia, J.N., Ji, H.Y., 2013. Recognition for cucumber disease based on leaf spot shape and neural network. Trans. Chinese Soc. Agric. Eng. 29 (S1), 115–121.

Cao, L.Y., Zhang, X.X., San, X.H., Chen, G.F., 2012. Research on the method of diagnosis for maize disease based on image processing technology and BP neural network algorithm. Comput. Sci. 39 (10).

Chouhan, S.S., Kaul, A., Singh, U.P., Jain, S., 2018. Bacterial foraging optimization based Radial Basis Function Neural Network (BRBFNN) for identification and classification of plant leaf diseases: an automatic approach towards Plant Pathology. IEEE Access. PP(99), 1.

Liu, L.B., Zhou, G.M., 2009. Identification method of rice leaf blast using multilayer perception neural network. Trans. Chinese Soc. Agric. Eng. 25 (S2), 13–217.

Zabalza, J., Clemente, C., Caterina, G.D., Ren, J.C., Soraghan, J.J., Marshall, S., 2014. Robust pca micro-doppler classification using svm on embedded systems. IEEE Trans. Aerosp. Electron. Syst. 50 (3), 2304–2310.

Zabalza, J., Ren, J.C., Yang, M.Q., Zhang, Y., Wang, J., Marshall, S., 2014. Novel folded-PCA for improved feature extraction and data reduction with hyperspectral imaging and SAR in remote sensing. ISPRS J. Photogramm. Remote Sens. 93 (7), 112–122.

Huang, M., Zhu, Q.B., Wang, B.J., Lu, R.F., 2012. Analysis of hyperspectral scattering images using locally linear embedding algorithm for apple mealiness classification. Comput. Electron. Agric. 89, 175–181.

Zhao, K.C., Shi, F.M., Meng, Q.L., Ma, L.G., 2013. Method of recognition of rice blast based on SVM. J. Northeast Agric. Univ. 44 (11), 118–126.

Qi, L., Ma, X., Zhang, X.C., 2006. Segmentation technology of color image about plant disease based on BP neural network. J. Jilin Univ. (Eng. Technol. Ed.) 36 (S2), 126–129.

Sha, C.S., Hou, J., Cui, H.X., 2016. A robust 2D Otsu's thresholding method in image segmentation. J. Vis. Commun. Image Represent. 41, 339–351.

Zhao, J.H., Luo, X.W., Zhou, Z.Y., 2008. Image segmentation method for sugarcane diseases based on color and shape features. Trans. Chinese Soc. Agric. Mach. 39 (9), 100–103.

Tang, J.T., Hu, D., Gong, Z.M., 2008. Research on the classification of SVM-based image texture features. Comput. Eng. Sci. 30 (8), 44–48.

Li, F., 2004. Principle of Regression Analysis Method and Practical Operation of SPSS.

China Financial Publishing House, Beijing.

Zhao, Q., Meng, D.Y., Xu, Z.B., 2014. Robust sparse principal component analysis. Sci. China (Inform. Sci.) 57 (9), 175–188.

Liu, J.F., 2014. Pattern recognition. Harbin Institute of Technology Press, Harbin, pp. 104–111.

Si, S.K., Sun, X.J., 2015. Mathematical Modeling. National Defense Industry Press, Beijing, pp. 406–407.

Ren, J.C., Zabalza, J., Marshall, S., Zheng, J., 2014. Effective feature extraction and data reduction with hyperspectral imaging in remote sensing. IEEE Signal Process Mag. 31 (4), 149–154.